Malaysian Journal Of Civil Engineering

NLFEM WITH HIGHER ORDER INTERPOLATION FUNCTION FOR EFFICIENT ANALYSIS OF IRREGULAR DOMAIN

M.A. Mohd Noor [a]*, M.H. Mokhtaram[b], M.Z. Jamil Abd Nazir [a], A.R. Zainal Abidin[a], A.Y. Mohd Yassin[c]

[a]Faculty of Civil Engineering, Universiti Teknologi Malaysia, 81310 UTM Johor Bahru, Johor, Malaysia
[b]Department of Engineering, Faculty of Engineering and Life Sciences, Universiti Selangor, 45600 Bestari Jaya, Selangor, Malaysia
[c]School of Energy, Geoscience, Infrastructure and Society, Heriot-Watt University Malaysia, 62200 Putrajaya, Malaysia

Article history
Received
12 April 2022
Received in revised form
06 July 2022
Accepted
07 July 2022
Published online
30 November 2022

*Corresponding author
maakhbar2@graduate.utm.my

Graphical abstract

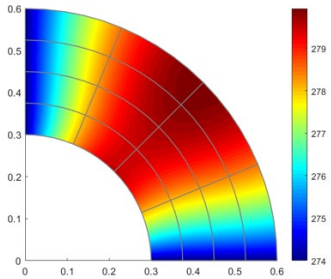

Abstract

This study proposes a new approach to developing a more efficient numerical technique by coupling the non-uniform rational B-spline (NURBS) with the higher-order polynomial basis functions under the framework of the Finite Element Method (FEM). In this technique, denoted as NURBS-Lagrange FEM (NLFEM), the NURBS basis functions are employed to represent the geometry of the problem domain, while the Lagrange interpolation functions are employed for the higher-order polynomial functions to interpolate the field variables. The NURBS is a mathematical model which provides a numerically stable algorithm to exactly represent all conic sections, and the Lagrange interpolation function allows for higher-order basis functions resulting in a faster convergence rate of analysis. By taking advantage of both models, the objective of this study is to propose a new approach, i.e., NLFEM, which can improve the accuracy of the analysis of the irregular domain with more efficient consumption of computer resources. A steady heat transfer formulation for a curved boundary problem is presented to demonstrate the validity and accuracy of the developed technique. The performance is verified against converged solutions obtained using higher-order FEM (FEM/Q9) and NURBS-Augmented FEM (NAFEM). The presented result shows that the NLFEM provides a favorable comparison against other methods. The converged solution is achieved 20% faster than the FEM/Q9 and 80 % faster than the NAFEM. This highlights the potential of the NLFEM as a new approach in numerical techniques for solving problems with irregular boundaries.

Keywords: FEM, NAFEM, NURBS, Lagrange interpolation function, Irregular domain

© 2022 Penerbit UTM Press. All rights reserved

1.0 INTRODUCTION

Finite Element Method (FEM) is a prominent numerical method for solving various engineering problems. The geometric approximation in FEM is achieved by employing piecewise polynomial interpolation functions. This can lead to accuracy issues, particularly when working with curvilinear geometries, as well as geometric imperfection-sensitivity issues. (Agrawal and Gautam, 2019; De Lazzari et al.,2021). Meanwhile, most commercial computer-aided design (CAD) software employs Non-Uniform Rational B-Spline (NURBS) to accurately represent complex geometry domains. (Wang et al.,2019). Hughes et al. (2005) proposed the idea of integrating NURBS into the analysis by introducing the concept of isogeometric analysis (IGA). The main idea of IGA is to use NURBS for both geometry representation and field variables. The three key work references for the IGA are Hughes et al. (2005), Bazilevs et al.

(2006), and Cottrell et al. (2006). Later, Cottrell et al. (2009) published a monograph devoted to IGA.

The NURBS basis function offers an efficient and numerically stable approach for precisely representing all curve boundaries and allows for flexible modelling. The properties of NURBS can be simply refined through the knot insertion, C^{p-1}-continuity. However, due to the non-interpolating properties of NURBS, special treatment is required for the imposition of the essential boundary conditions (Agrawal and Gautam, 2019; Mishra and Barik, 2020). Several other challenges faced by IGA, such as local refining, volumetric mesh generation and trimmed NURBS, have also been addressed (Cottrell et al., 2009; Lu et al.,2013; Pantaleón, 2014). A significant number of studies for combining NURBS with existing numerical methods like as FEM, Meshfree, and Finite Volume Method have been reported, with promising results. (Heinrich and Simeon, 2012; Legrain, 2013; Safdari et al., 2015; Chi and Lin, 2016; Meng and Hu, 2018; Nguyen et al., 2022).

NURBS-Enhanced Finite Element Method (NEFEM) was presented by Sevilla et al. (2008a, 2008b, 2011) to improve the classical FEM. In NEFEM, the NURBS was used to represent the curved boundary and the solution is approximated using the standard piecewise polynomials interpolation function. Standard FE interpolation is employed for elements that do not intersect with the curve boundary. By using NURBS for the boundary domain description, NEFEM is able to precisely represent the geometry. The study showed that NEFEM was at least one order more precise than using the isoparametric element in the classical FEM. The ability to obtain an accurate solution with course mesh makes NEFEM much more computationally efficient than classical FEM (Make et al.,2020). However, for the elements that intersect with the NURBS boundary, a specially constructed piecewise interpolation is required. As a result, fully automatic mesh generation for NEFEM required a special scheme to fully exploit its potential. (Sevilla et al., 2016).

NURBS-Augmented Finite Element Method (NAFEM) is another variant of the NURBS coupling with the FEM framework. It was proposed for plate with complex geometries by Mishra and Barik (2019, 2020, 2021). Unlike NEFEM, NAFEM uses NURBS for complete geometry description and adopts the standard finite element basis function for variable fields. The key advantages of NAFEM rely on the simple enforcement of the essential boundary conditions as compared to IGA. Moreover, NAFEM is much more flexible due to its ability to break the complex geometry into more amenable patches. The results of NAFEM have been found to be in excellent agreement with classical FEA and NEFEM.

In recent years, Meshfree techniques have been developed and have made significant progress. Meshfree methods were developed in an effort to eliminate the necessity of predefined meshes that are essential in FEM by introducing higher-order interpolation to discretize the domain. Several studies have been made to couple the Meshfree technique with NURBS, of which Rosolen and Arroyo were among the first to make an effort (2013). The method was then applied to situations involving time-harmonic acoustics (Greco, et al., 2016; Greco, et al., 2017). Mokhtaram, et al. (2020) enhanced the coupled formulation with interpolatory meshless shape functions, and radial basis functions (RBF) to improve the imposition of boundary conditions.

However, coupled NURBS and Meshfree techniques face instability when a large number of nodes need to be fitted. The probability of an ill-conditioned moment matrix might result in singularity issues during matrix inversion. Another drawback is no established optimal value for all related shape parameters involved in Meshfree techniques. These values are typically pre-determined by the analyst and confirmed through a series of numerical tests.

In this study, to fully utilize the advantages of coupled NURBS and FEM, another variant called NURBS-Lagrange Finite Element Method (NLFEM) is proposed. In NLFEM, NURBS are employed to represent the domain boundary while a higher-order polynomial function is used to approximate the field variables. In contrast to NAFEM, NLFEM employs the concept of a higher-order polynomial function by using the Lagrange interpolation function. To strengthen the idea of the method developed, studies have been conducted for a steady heat transfer with curved boundaries problem.

The following is an outline of the paper: Section 2 describes the formulation of NURBS basis function. In Section 3, the formulation of FEM for steady heat transfer is presented. The coupling scheme is detailed in Section 4, which is the primary focus of the study. Section 5 includes a numerical example to highlight the performance and the advantages of the proposed method. Section 6 summarises and concludes the study.

2.0 FORMULATION OF NURBS BASIS FUNCTION

The NURBS are constructed from B-spline. The B-spline basis function is defined by a set of one-dimensional coordinates in the parameter space known as knot vector, $\Xi = \{\xi_1, \xi_2, \dots, \xi_{n+p+1}\}$ where ξ_i is the *i*-th knot value, *n* and p is the number of basis function and the polynomial order respectively. The term 'order' of polynomial is also referred as 'degree' in computational geometry literature. The order of $p = 0,1,2,3$ and therefore on refer to constant, linear, quadratic, cubic and so forth.

Using Cox-de-Boor recursion formula, the B-spline function in one dimensional starting with constants, $p = 0$ can be written as.

$$N_{i,0}(\xi) = \begin{cases} 1, & \text{if } \xi_i \le \xi < \xi_{i+1} \\ 0, & \text{otherwise} \end{cases} \tag{1}$$

$$N_{i,p}(\xi) = \frac{\xi - \xi_i}{\xi_{i+p} - \xi_i} N_{i,p-1}(\xi) + \frac{\xi_{i+p+1} - \xi}{\xi_{i+p+1} - \xi_{i+1}} N_{i+1,p-1}(\xi) \tag{2}$$

The basis function of 1D NURBS can be written as follows;

$$R_i^p(\xi) = \frac{N_{i,p}(\xi) w_i}{\sum_{i=1}^{n} N_{i,p}(\xi) w_i} \tag{3}$$

where w is non-negative weight.

In 2D, the basis function is defined by the result of the NURBS tensor in ξ and η. It is represented by a $n \times m$ control points,

two polynomial degrees (p and q), two-knot vectors (Ξ and $\mathcal{H}$), and two corresponding basis functions ($N_{i,p}$ and $M_{j,q}$) in ξ- and η- directions respectively. The basis function can be written as follows;

$$R_{i,j}^{p,q}(\xi,\eta) = \frac{N_{i,p}(\xi)M_{j,q}(\eta)w_{i,j}}{\sum_{i=1}^{n}\sum_{j=1}^{m}N_{i,p}(\xi)M_{j,q}(\eta)w_{i,j}} \tag{4}$$

A NURBS surface $S^n(\xi,\eta)$ can then be defined as;

$$S^n(\xi,\eta) = \sum_{i=1}^{n}\sum_{j=1}^{m}R_{i,j}^{p,q}(\xi,\eta)\,\boldsymbol{B_{i,j}} \tag{5}$$

where B is the coordinate of the control-point.

Figure 1 illustrates the weight, w of NURBS control points, B of a circle formed by (a) quarter arcs and (b) one-third arcs. The weights of the control points which intersect with the circle's boundary, *i.e.*, P_1, P_3, P_5, P_7, P_9 at Figure 1 (a) and P_1, P_3, P_5, P_7 at Figure 1 (b), are 1, while the remaining control is $1/\sqrt{2}$ at P_2, P_4, P_6, P_8 for quarter arcs and $1/2$ at P_2, P_4, P_6 for one-third arcs.

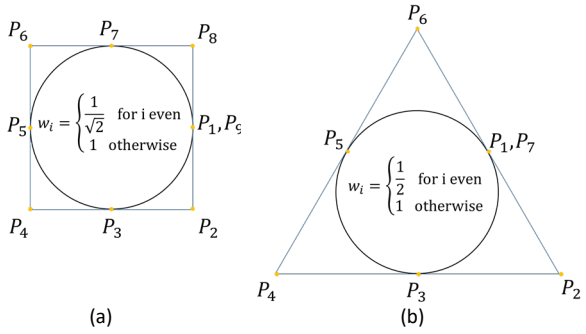

Figure 1 Weight for a circle built formed by (a) quarter arcs and (b) one-third arcs.

3.0 FORMULATION OF FEM FOR STEADY HEAT TRANSFER

This section presents a FEM formulation for a 2-D steady heat transfer problem. The Lagrange shape functions are used to approximate the interest variables.

3.1 Lagrange Interpolation Functions

The linear finite element solution of the interest variables, $u(x)$ for n number of degree of freedom (dof) are written as follow;

$$U(x) = \sum_{i=1}^{n}L_i(x)u_i \tag{6}$$

The L_i is Lagrange interpolation function for a polynomial of degree n-1 and u_i is the nodal dof. The Lagrange interpolation can be computed by following formula;

$$L_i(x) = \prod_{\substack{j=1\\ j\neq i}}^{n}\frac{x-x_j}{x_i-x_j} \tag{7}$$

Symbol $\prod$ indicates a product of terms. Since the product of Equation (7) includes all term except the i-th, hence there are $n-1$ terms. For 2D elements, Lagrange interpolation can be obtained by taking the tensor product of 1-D Lagrange. The interpolation of variables of Equation (6) can be written as;

$$U(x,y) = \sum_{i=1}^{n}\sum_{j=1}^{n}L_{i,j}(x,y)u_{i,j} \tag{8}$$

and a bilinear Lagrange interpolation as;

$$L_{i,j}(x,y) = L_i(x)L_j(y) \tag{9}$$

3.2 Galerkin Weak Form of Steady Heat Transfer

The steady heat transfer partial differential equation (PDE) is written as follows;

$$\frac{\partial}{\partial x}\left(k_x\frac{\partial T}{\partial x}\right)+\frac{\partial}{\partial y}\left(k_y\frac{\partial T}{\partial y}\right) = -Q \tag{10}$$

T and Q represent the internal temperature and heat generation, respectively. The thermal conductivity in the x and y directions is denoted by k_x and k_y, respectively. The standard Galerkin weak formulation of Equation (10) can be presented in matrix form as;

$$\int_{\Omega}\{L\}^T\{\partial\}[E]\{\partial\}^T\{L\}\{T\}^T d\Omega = \int_{\Omega}\{L\}^T q_H d\Omega + \int_{s}\{L\}^T\{b\}^T ds \tag{11}$$

where

$[E] = \begin{bmatrix}k_x & 0\\ 0 & k_y\end{bmatrix}$ is the constitutive matrix.

$\{\partial\} = \left\{\frac{\partial}{\partial x} \quad \frac{\partial}{\partial y}\right\}$ is the differential operator matrix.

L is Lagrange interpolation function as derived in section 3.1. Equation (11) can be generalized as follows;

$$[K]\{T\}^T = \{q\}+\{b\} = \{R\} \tag{12}$$

where,

$$[K] = \int_{\Omega} \{L\}^T \{\partial\}[E]\{\partial\}^T \{L\} d\Omega \tag{13}$$

$$\{q\} = \int_{\Omega} \{L\}^T q_H d\Omega \tag{14}$$

$$\{b\} = \int_{s} \{L\}^T \{b\}^T ds \tag{15}$$

$[K]$ denotes the stiffness matrix, whereas vectors $\{T\}$ and $\{R\}$ denote the degree of freedom (DOF) and the loading, respectively.

4.0 COUPLED FORMULATION OF NURBS-FEM WITH HIGHER ORDER INTERPOLATION FUNCTION

The proposed method employed NURBS for geometry representation and higher-order polynomial functions for field variables to improve accuracy and convergence rate. In contrast to conventional Isoparametric elements in FEM, the use of NURBS for geometrical representation requires the introduction of a new mapping space known as parametric space. This is the NURBS mapping's pre-image. The parametric coordinates are defined as $(\hat{\xi}, \hat{\eta}) \in \widehat{\Omega}$ with the domain limit, $\widehat{\Omega} = [0,1]$. There are two layers of mapping that must be addressed when implementing parametric space mapping. Figure 2 indicates the mapping from parent into parametric space $\phi^e: \widetilde{\Omega} \longrightarrow \widehat{\Omega}^e$ and parametric space into physical space $F: \widehat{\Omega} \rightarrow \Omega$.

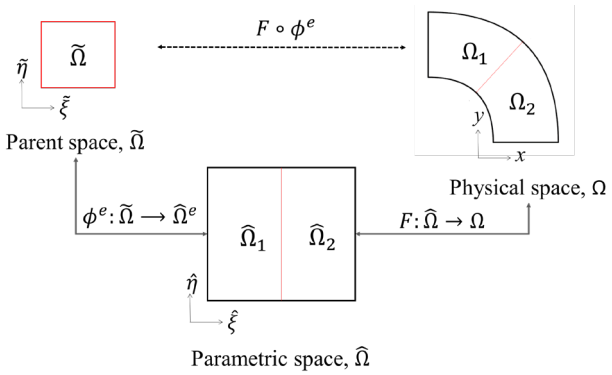

Figure 2 Mapping of the problem domain using NURBS

Numerical integration is conducted in parent space in the same manner as conventional FEM for isoparametric elements. Thus, geometric mapping is used to transform the physical domain into parametric space, and subsequently, affine mapping is used to transform it further into parent space. These double mappings can be expressed mathematically as follows;

$$\int_{\Omega} f(x,y) d\Omega = \sum_{e=1}^{n} \int_{\Omega_e} f(x,y) d\Omega_e$$

$$= \sum_{e=1}^{n} \int_{\widehat{\Omega}_e} f\left(x(\hat{\xi}), y(\hat{\eta})\right) |J_{\hat{\xi}}| d\widehat{\Omega}_e$$

$$= \sum_{e=1}^{n} \int_{\widetilde{\Omega}_e} f(\tilde{\xi}, \tilde{\eta}) |J_{\tilde{\xi}}| |J_{\tilde{\xi}}| d\widetilde{\Omega}_e \tag{16}$$

The stiffness matrix formerly defined by Equation (13), will now be expressed as follows;

$$[K] = \sum_{k}^{n_c} \sum_{i=1}^{n_g} \widetilde{w} \{L\}^T \{\partial\}[E]\{\partial\}^T \{L\} |J_{\tilde{\xi}}| |J_{\tilde{\xi}}| \tag{17}$$

where n_g and n_c is the number of gauss points and elements respectively. $\widetilde{w}$ is the corresponding weights of the Gauss quadrature.

Equation (17) can be rewritten as follows;

$$[K] = \sum_{k}^{n_c} \sum_{i=1}^{n_g} \widetilde{w} [B]^T [E][B] |J_{\tilde{\xi}}| |J_{\tilde{\xi}}| \tag{18}$$

where $[B]$ is the strain-displacement matrix, given as;

$$[B] = J_{\tilde{\xi}}^{-1} J_{\tilde{\xi}}^{-1} [\tilde{B}] \tag{19}$$

The Jacobian for four-node rectangular element and a NURBS for affine mapping is denoted by $J_{\tilde{\xi}}$ and $J_{\tilde{\xi}}$, respectively.

5.0 NUMERICAL EXAMPLE

This section validates the proposed formulation and investigates the performance of the approach in dealing with irregular boundary. A steady heat transfer problem with an inner radius of 0.3 and an outside radius of 0.6 is chosen. **Figure 3** illustrates the problem domain in parametric space and physical space, respectively.

The temperature, T at Γ_1 and Γ_3 is $274\ K$ while the internal heat generation, Q is $2 \times 10^4\ W/m^3$. The boundary heat flux, q at Γ_2 are $1 \times 10^3\ W/m^2$. The thermal conductivity, k_x and k_y is $237\ W/mK$.

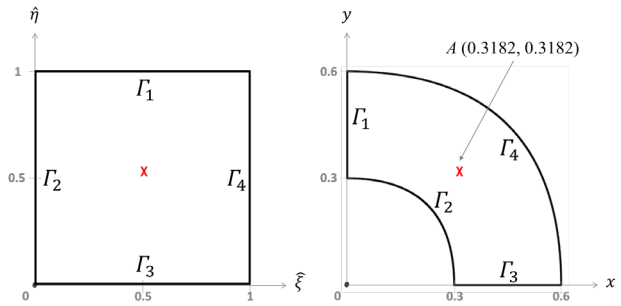

Figure 3 The domain in (a) parametric space and (b) physical space

Based on the domain depiction in Figure 3, the lowest polynomial order, $p = 1$ is chosen for straight boundaries and $q = 2$ for curve boundaries. The knot vectors used to determine the number of knot spans, whereas the knot values dictate the number of elements in the patches. The continuity of basis function across the element boundaries is reduced by repeating the knot values.

Table 1 tabulated the relevant parameters for three types of models used in this study, while Figure 4 depicts the associated elements and control points of each model.

Table 1 Parameter for model A, B and C

Models	-direction	Polynomial order	Control point	Knot Vectors	Total control Point ($n \times m$)	Number of Elements
A	$\hat{\xi}$	p = 1	n = 2	Ξ = {0,0,1,1}	6	1×1
	$\hat{\eta}$	q = 2	m = 3	H = {0,0,0,1,1,1}		
B	$\hat{\xi}$	p = 1	n = 5	Ξ = {0,0,0.25,0.5,0.75,1,1}	30	4×4
	$\hat{\eta}$	q = 2	m = 6	H = {0,0,0, 0.25,0.5,0.75,1,1,1}		
C	$\hat{\xi}$	p = 1	n = 9	Ξ = {0,0,0.125,0.25,0.375,0.5,0.625,0.75,0.875,1,1}	90	8×8
	$\hat{\eta}$	q = 2	m = 10	H = {0,0,0, 0.125,0.25,0.375,0.5,0.625,0.75,0.875,1,1,1}		

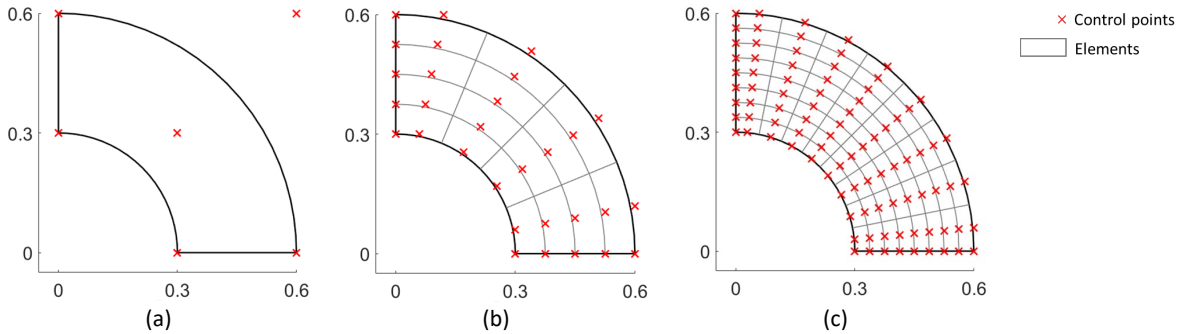

Figure 4 Physical geometry and number of elements for (a) Models A (b) B and (c) C

6.0 RESULTS AND DISCUSSION

The main interest of this study is to analyse the efficiency of coupled NURBS and FEM by using higher-order terms in the shape function, *i.e.*, the Lagrange interpolation function. The performance of the purposed method is evaluated by the convergence rates of the results. The convergence error is plotted, and the lowest errors at the fewest nodes are considered to converge faster and perform better.

6.1 Convergence Rate of Area

A preliminary study begins with the comparison of the area convergence rates employing the NURBS and the FEM, *i.e.*, conventional FEM (FEM/Q4) and higher-order FEM (FEM/Q9) as shown in Figure 5. The purpose of the comparison is to demonstrate the advantages of NURBS for representing curve boundaries.

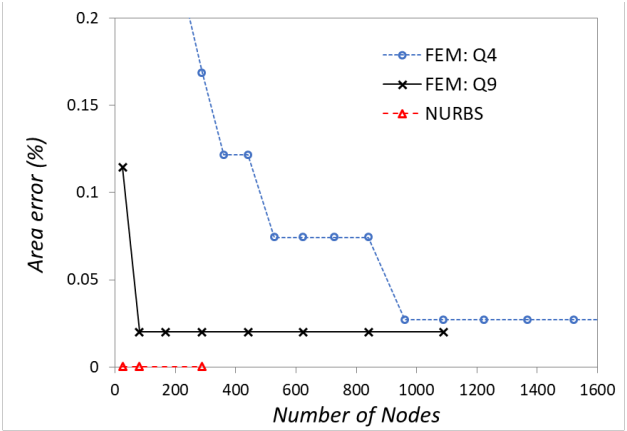

Figure 5 Convergence of area error

Figure 5 shows that the NURBS basis function is able to provide an exact area with a very few nodes followed by FEM/Q9, then FEM/Q4. The higher convergence error rate by FEM is due to the piecewise polynomial used to represent the irregularity of the problem domain, where for better accuracy,

FEM requires more elements to define the curve boundaries. This indicates the coupled NURBS in the FEM framework has significantly benefited the mapping of curved boundaries, resulting in more reliable results, and substantial time savings throughout the meshing process.

6.2 Convergence Rate of Temperature

As this study focuses on the development of a new technique, *i.e.*, NLFEM, the main interest is to compare the performance of the developed technique with other methods based on the FEM framework, *i.e.*, FEM/Q4, FEM/Q9 and NAFEM. The variable of interest is compared at Point A which has the coordinates (0.3182, 0.3182) in physical space and the midpoint of the domain in parameter space as illustrated in **Figure 3**. It should be noted that, since there is no closed-form solution available for the problem given, the exact solution herein is defined from COMSOL Multiphysics, a commercial FEM software, with a very fine mesh. Based on the software analysis, the exact temperature at Point A is assumed to be $279.65\ K$.

The higher-order interpolation exhibits Runge's phenomenon in turn disrupting the stability and accuracy of the results, therefore in the developed method, the polynomial order arrangement is controlled by the presence of a knot span. Three models have been used in the arrangement, *i.e.*, Model A with a 1x1 knot span, Model B with a 4x4 knot span, and Model C with an 8x8 knot span. Figure 6 shows the temperature convergence error at point A for the three models.

Figure 6 shows that models B and C provide an exact solution, whereas model A with a single knot span produces a significant error as the number of nodes increases. Therefore, in order to maintain a balance between accuracy and stability of the results, the density of nodes within the problem domain has been controlled by the number of knot spans.

Figure 7 compares the performance of the NLFEM against the conventional FEM, FEM/Q4 and FEM/Q9, as well as the established couple formulations of NURBS and FEM, *i.e.* NAFEM.

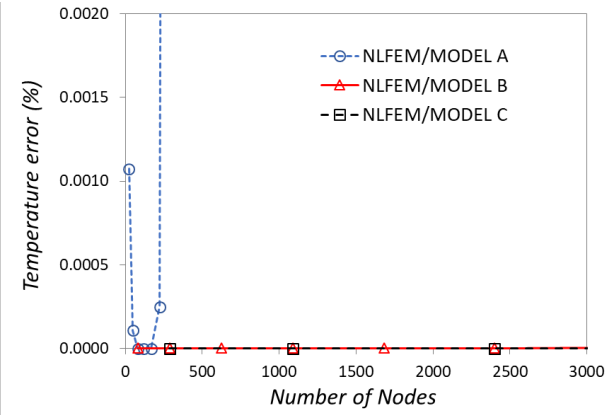

Figure 6 Convergence rate of the temperature error at point A for Model A with a 1x1 knot span, Model B with a 4x4 knot span and Model C with an 8x8 knot span

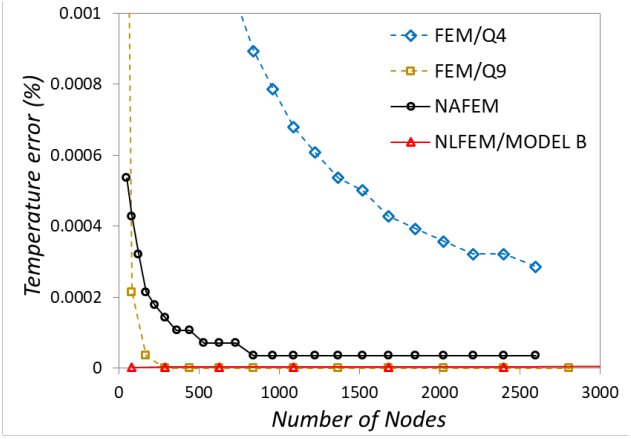

Figure 7 Convergence rate of temperatures

The figure shows that the higher-order interpolation functions, *i.e.*, FEM/Q9 and NLFEM, result in a nearly exact solution. Of the two, NLFEM provides better performance by having a faster convergence rate. It can be seen that the idea of enhanced conventional higher-order FEM with NURBS, *i.e.*, NLFEM, has proven to work better with a much smaller number of nodes than FEM/Q9, which requires close to 500 nodes to converge.

6.3 Computer Resource Consumption

All of these techniques are also assessed in terms of computer resource consumption with respect to temperature accuracy and the number of nodes as shown in **Figure 8**. It refers to how much time takes for a computer to complete a process for a given set of input and given set of output. It should be noted that for better comparison, all algorithms are developed based on the author's source code, where the similarity of the algorithm is retained in the main source code.

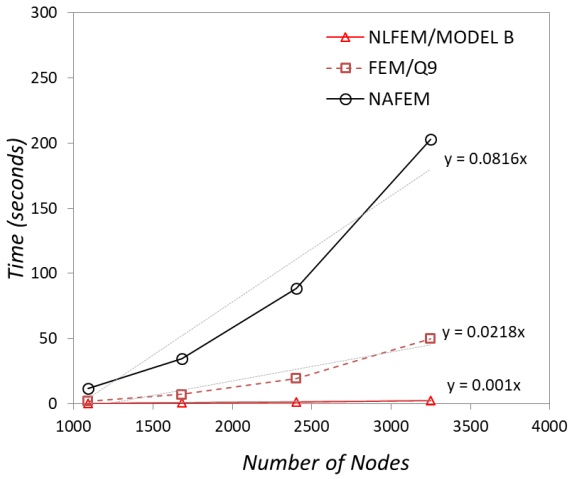

Figure 8 Computing time consumed for NLFEM/MODEL B, FEM/Q9 and NAFEM with different number of nodes

From Figure 8, it can be observed that after 1000 nodes, the NAFEM consumes a remarkably higher computer resource consumption with approximately 0.0816 linear slope followed by FEM/Q9 with approximately 0.028 linear slope. The

NLFEM/Model B consumes the best computer resource consumption where the converged solution is achieved approximately 20 % faster than the FEM/Q9 and 80 % faster than NAFEM. This result indicates that the higher-order polynomial basis function performs better in terms of computer resources compared to the coupled conventional FEM and NURBS, *i.e.*, NAFEM, and the performance shows excellent improvement with NURBS coupling. This is due to less number of nodes used in the geometric modelling thus accelerating the use of time throughout the process. Such validation suggests that this new technique, *i.e.*, NLFEM, promises a highly effective solution when dealing with irregular domain problems.

Temperature field comparisons between NLFEM and COMSOL Multiphysics are shown in Figure 9

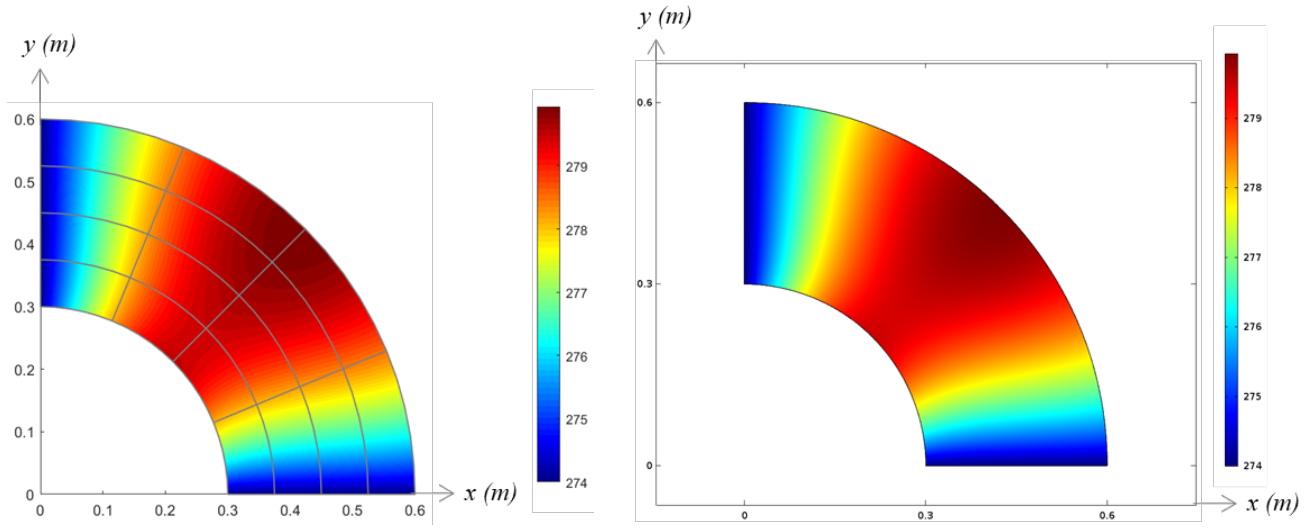

(a) (b)

Figure 9 Comparison of temperatures using (a) NLFEM Model B and (b) COMSOL

7.0 CONCLUSIONS

This paper presents a new numerical method to promote the integration of NURBS and FEM in the analysis of irregular domain problems. In this method, *i.e.*, NLFEM, the field variables are approximated using the Lagrange interpolation function, while the problem domains are mapped using the NURBS basis function to represent the geometry exactly. The method is formulated under the FEM framework. A step-by-step procedure for the development of the method has been detailed.

In assessing the performance of the proposed method, a steady heat transfer problem with an irregular boundary has been analyzed. Tests have been carried out on the analysis of convergence rate. In all tests, NLFEM performs better than other methods, *i.e.*, FEM/Q4, FEM/Q9 and NAFEM, where the NLFEM always converge faster. It consumes the best computer resource consumption where the converged solution is achieved approximately 20 % faster than the FEM/Q9 and 80 % faster than NAFEM. This highlights the potential of the method as an alternative method for numerical analysis of irregular domain problems. This method improves the existing numerical method in the following ways: preserve the main feature of FEM that is the stability and versatility in the imposition of essential boundary conditions, improves the accuracy of the geometric mapping by the NURBS basis functions, and increases the convergence rate of analysis by the higher-order polynomial basis functions.

Acknowledgements

This study was conducted as part of the requirements for a PhD programme at Universiti Teknologi Malaysia. It was funded through MyPhD initiative by Kementerian Pendidikan Malaysia and also supported by the Universiti Teknologi Malaysia (Research grant no. Q.J130000.2551.21H01).

References

[1] Agrawal, V., & Gautam, S. S. 2019. IGA: a simplified introduction and implementation details for finite element users. *Journal of The Institution of Engineers (India): Series C*, 100(3): 561-585.

[2] Bazilevs, Y., Beirao, L., Veiga, D., Cottrell, J., Hughes T.J.R., and Sangalli, G. 2006. Isogeometric analysis: approximation, stability and error estimates for h-refined meshes. *Mathematical Models and Methods in Applied Sciences*, 16: 1031-1090.

[3] Chi, S. W., & Lin, S. P. 2016. Meshfree analysis with the aid of NURBS boundary. *Computational Mechanics*, 58(3): 371-389.

[4] Cottrell, J.A., Hughes, T.J.R. and Bazilevs, Y. 2009 I*sogeometric analysis toward integration of CAD and FEA*. John Wiley and Sons.

[5] Cottrell, J.A., Reali, A., Bazilevs, Y. and Hughes, T.J.R. 2006. Isogeometric analysis of structural vibrations. *Computer Methods in Applied Mechanics and Engineering*, 195: 5257-5296.

[6] De Lazzari, E., van den Boom, S. J., Zhang, J., van Keulen, F., & Aragón, A. M. 2021. A critical view on the use of Non-Uniform Rational B-Splines to improve geometry representation in enriched finite element methods. I*nternational Journal for Numerical Methods in Engineering*, 122(5): 1195-1216.

[7] Greco, F., Coox, L., & Desmet, W. 2016. Maximum-entropy methods for time-harmonic acoustics. *Computer Methods in Applied Mechanics and Engineering*, 306: 1-18.

[8] Greco, F., Coox, L., Maurin, F. and Desmet, W. 2017. NURBS-enhanced maximum-entropy schemes. *Computer Methods in Applied Mechanics and Engineering,* 317: 580–97.

[9] Heinrich, C., & Simeon, B. 2012. A finite volume method on NURBS geometries and its application in isogeometric fluid–structure interaction. *Mathematics and Computers in Simulation,* 82(9): 1645-1666.

[10] Hughes, T.J.R., Cottrell, J.A., and Bazilevs, Y. 2005. Isogeometric analysis: CAD, finite elements, NURBS, exact geometry and mesh refinement. *Computer Methods In Applied Mechanics And Engineering* 194: 4135–4195.

[11] Legrain, G. 2013. A NURBS enhanced extended finite element approach for unfitted CAD analysis. *Computational Mechanics*, 52(4): 913-929.

[12] Lu, J., Yang, G., & Ge, J. 2013. Blending NURBS and Lagrangian representations in isogeometric analysis. *Computer Methods in Applied Mechanics and Engineering*, 257: 117-125.

[13] Make, M., Hosters, N., Behr, M., & Elgeti, S. 2020. Space-Time NURBS-Enhanced Finite Elements for Solving the Compressible Navier–Stokes Equations. I*n Numerical Methods for Flows.* 97-107.

[14] Meng, X., & Hu, G. 2018. A NURBS-enhanced finite volume solver for steady Euler equations. *Journal of Computational Physics,* 359: 77-92.

[15] Mishra, B. P., and Barik, M. 2018. NURBS-augmented finite element method for stability analysis of arbitrary thin plates. Engineering with Computers., 35(38):1-12.

[16] Mishra, B. P., and Barik, M. 2020. NURBS-Augmented Finite Element Method for static analysis of arbitrary plates. C*omputers and Structures.*, 232.

[17] Mishra, B. P., & Barik, M. 2021. Free flexural vibration of thin stiffened plates using NURBS-Augmented finite element method. In *Structures* 33: 1620-1632.

[18] Mokhtaram, M. H., Mohd Noor, M. A., Jamil Abd Nazir, M. Z., Zainal Abidin, A. R., and Mohd Yassin, A. Y. 2020. Enhanced meshfree RPIM with NURBS basis function for analysis of irregular boundary domain. *Malaysian Journal of Civil Engineering* 32(1): 19–27.

[19] Nguyen, N. T., Nguyen, M. N., Van Vu, T., Truong, T. T., & Bui, T. Q. 2022. A meshfree model enhanced by NURBS-based Cartesian transformation method for cracks at finite deformation in hyperelastic solids. *Engineering Fracture Mechanics,* 261: 108176.

[20] Pantaleón, C. (2014). Applications of Isogeometric Analysis Coupled with Finite Volume Method. Rochester Institute of Technology.

[21] Rosolen, A. and Arroyo, M. (2013). Blending isogeometric analysis and local maximum entropy meshfree approximants. *Computer Methods in Applied Mechanics and Engineering*, 264: 95–107.

[22] Safdari, M., Najafi, A. R., Sottos, N. R., & Geubelle, P. H. 2015. A NURBS-based interface-enriched generalized finite element method for problems with complex discontinuous gradient fields. *International Journal for Numerical Methods in Engineering,* 101(12): 950-964.

[23] Sevilla, R., Fernandez-Mendez, S., & Huerta, A. 2008a. NURBS-enhanced finite element method (NEFEM). *International Journal for Numerical Methods in Engineering*, 76: 56-83.

[24] Sevilla, R., Fernandez-Mendez, S., & Huerta, A. 2008b. NURBS-enhanced finite element method for Euler equations. *International Journal for Numerical Methods in Fluids*, 57:1051–1069.

[25] Sevilla, R., Fernández-Méndez, S., & Huerta, A. 2011. 3D NURBS-enhanced finite element method (NEFEM). *International Journal for Numerical Methods in Engineering*, 88(2): 103-125.

[26] Sevilla, R., Rees, L., & Hassan, O. (2016). The generation of triangular meshes for NURBS-enhanced FEM. *International Journal for Numerical Methods in Engineering*, 108(8): 941-968.

[27] Wang, Q., Zhou, W., Cheng, Y., Ma, G., Chang, X., & Liu, B. 2019. A NURBS-enhanced improved interpolating boundary element-free method for 2D potential problems and accelerated by fast multipole method. *Engineering Analysis with Boundary Elements,* 98: 126-136.